Journal of The Electrochemical Society, **153** (7) B253-B259 (2006)
0013-4651/2006/153(7)/B253/7/$20.00 © The Electrochemical Society

Development of an Electroless Method to Deposit Corrosion-Resistant Silicate Layers on Metallic Substrates

Swaminatha P. Kumaraguru, Basker Veeraraghavan, and Branko N. Popov[*,z]

Center for Electrochemical Engineering, Department of Chemical Engineering, University of South Carolina, Columbia, South Carolina 29208, USA

A novel electroless method for depositing corrosion-resistant silicate layers on metallic substrates from aqueous solutions has been developed. The silicate layer was deposited from an aqueous solution of sodium silicate (3.22 weight ratio sodium silicate, 37.5% solution in water from PQ Corporation) and sodium borohydride. The technique is demonstrated by forming a passive film on galvanized steel. Deposition parameters such as concentration of the bath, temperature, and pH have been optimized based on the corrosion characteristics of the final coating. Studies on the coating reveal the formation of a very thin (5 nm) zinc disilicate layer followed by a much thicker (500 nm) silica layer. Accelerated corrosion tests showed that the silicate coatings have higher corrosion resistance and better stability when compared to chrome passivates. Silica coatings developed by this method show promise as an alternative to chrome passivation for corrosion protection.

[DOI: 10.1149/1.2201549]

Manuscript submitted January 5, 2006; revised manuscript received March 22, 2006. Available electronically May 17, 2006.

Phosphate and chromate-based conversion coatings are widely used to decrease the dissolution of sacrificial deposits such as Zn and Zn alloys.[1-3] Among them, chrome passivates are widely preferred due to their high corrosion resistance, barrier, and self-healing properties, and the ease with which they are applied. However, chrome passivates are generally prepared from hexavalent chromium-based bath, which is known for its toxicity.[4] Governing bodies such as the Environmental Protection Agency and the European Union have issued stringent regulations for the use of hexavalent chromium and its salts in automobiles to facilitate recycling. Several chrome alternatives are currently explored worldwide.[5,6]

Soluble silicates are economical and environmentally friendly and have been used for several decades to protect metals.[7] They form a thin protective film on various metal surfaces. Corrosion-resistant coating of colloidal silica along with hexavalent and trivalent chromium was developed as early as 1972.[8] Steel was quenched in silica solution to form a thin layer of the coating.[9] However, the formation of a stable and uniform silica coating for corrosion protection remains a challenge and has been actively investigated. Deposition of silica films has been accomplished previously by several methods including sol-gel deposition,[10] precipitation,[11] and through electrolysis at high voltages.[12-14] Cheng et al.[10] developed an aluminosilicate coating through a sol-gel process in autoclave at 175°C. Jesionowski[11] prepared colloidal silica by precipitation of silicate solution using sulfuric acid in emulsion medium. Speers and Cohoon[12] report the anodic deposition of silica from alkaline silicate electrolytes by anodizing aluminum at 350 V. This process is limited to Al or similar metals which have stable anodic oxide films and involves application of large potentials. Recently, Chigane et al.,[13] prepared thin films of silica from aqueous fluoride electrolytes by electrolysis. However, all these processes are not suited for commercial applications due to either their time-intensive nature or due to the poor quality of silica films formed. Previously,[14] we have reported the optimization of an electrolytic process by which silica can be electrodeposited at the cathode. It was found that corrosion-resistant silica films can be deposited from a dilute sodium silicate solution at an applied voltage of 12 V. It has been shown that hydrogen evolution and removal of water at the interface favor silica deposition. A postheating step at 175°C was found to increase the corrosion resistance and performance of the coatings. Also, Dalbin et al. reported silica deposition by immersion followed by heat-treatment at 120°C.[15] These processes are energy-intensive due the post-heat-treatment step at 120°C for 2 h and are not commercially viable. In the absence of a heat-treatment step, the silica adhered on the substrate dissolves rapidly in aqueous media.

In the present paper, we summarize our findings on the development of a novel electroless method to replicate the electrolytic process without any heat-treatment for the deposition of silica coatings. Uniform and adherent silicate layers were deposited by the electroless method which involves a single immersion step in the electroless bath followed by drying at room temperature. The electroless process does not involve electrochemical reduction of any silicate species; silica deposition was obtained by water removal at the metal–electrolyte interface. The process described here is general in nature and can be applied to a wide variety of metals. Further, it is inexpensive and the entire process is environmentally benign. Also, the naturally available hemimorphite form of zinc disilicate has been found to be reproduced through this process.

Experimental

Silica depositions were performed on galvanized steel panels (EZG-60G) with surface area 116 cm^2 on each side, as received from ACT labs. Zinc was deposited on steel substrate at room temperature using current density of 30 mA/cm^2. The bath contained 300 g/L $ZnSO_4$, 30 g/L $ZnCl_2$, and 30 g/L H_3BO_3, pH 4. The thickness of the zinc deposit was 10 μm. Prior to silica deposition, the galvanized steel samples were degreased with acetone and washed with demineralized water. A sodium silicate solution (37.5 wt % silicic acid, sodium salt in 62.5 wt % water) with a SiO_2/Na_2O ratio of 3.22 obtained from PQ Corporation was used as a silicate precursor. Electroless deposition of silica was performed from a diluted solution of sodium silicate with a known concentration of sodium borohydride ($NaBH_4$). The experimental study consisted of optimizing the bath parameters such as concentration of the sodium silicate, sodium borohydride in the electrolyte, pH, and bath temperature.

The corrosion characteristics of all panels were evaluated in 0.5 M Na_2SO_4 solution at pH 4.0. A three-electrode setup was used to study the corrosion behavior of the mineralized samples. The panel under study served as the working electrode. Pt was used as a counter electrode and a standard calomel electrode (SCE) as a reference electrode. After the open-circuit potential stabilized, nondestructive evaluation of the coating was done using linear polarization technique. The potential was applied 10 mV above and below the open-circuit potential at a scan rate of 0.1667 mV/s. All measurements were performed with an EG&G PAR model 273A potentiostat interfaced with a computer. Accelerated corrosion testing was carried out using an Atotech environmental test chamber model P22E001. The samples were exposed to a constant 5% salt fog in accordance with the ASTM B-117 specifications. The appearance of

---

[*] Electrochemical Society Active Member.
[z] E-mail: popov@engr.sc.edu

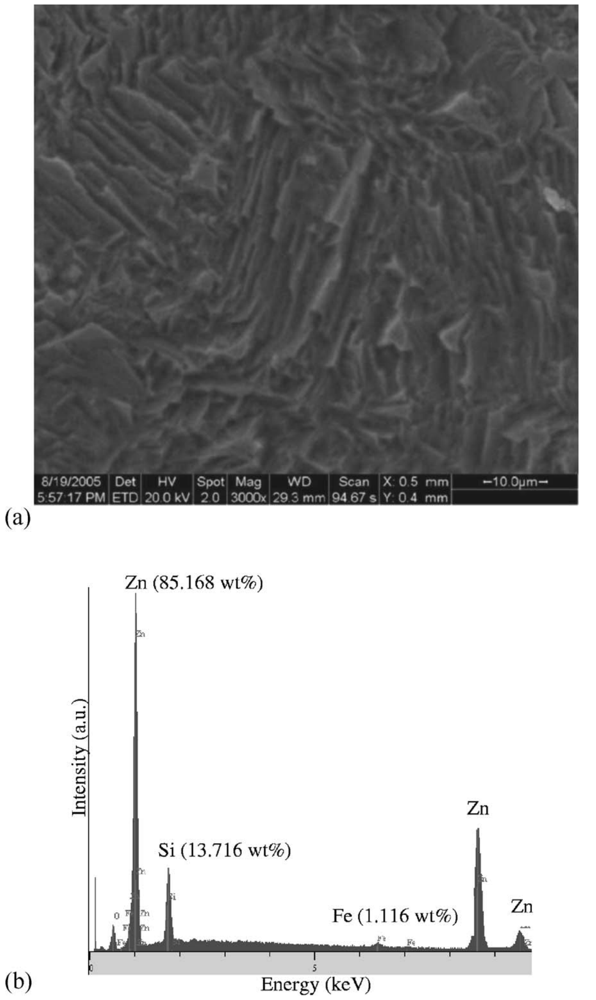

Figure 1. (a) SEM and (b) EDAX spectrum of galvanized steel coated with silica.

the white rust, red rust, and the failure of the samples were observed as a function of time. The basis for the failure criterion was determined as 5% red rust on the surface of the samples.

Surface morphology of the coatings was analyzed by viewing them under an ESEM FEI Quanta 200 micrsoscope. Constitutive elements on the surface of the panels were analyzed using energy-dispersive analysis with X-rays (EDAX). X-ray photoelectron spectroscopy (XPS), also known as electron spectroscopy for chemical analysis (ESCA), was used to analyze the nature of the coating. ESCA results were obtained using a Hewlett-Packard 5950 A ESCA spectrometer which is capable of generating monochromator X-rays at a background pressure of $<5 \times 10^{-9}$ Torr. The ability of ESCA to generate accurate binding energies is reflected by these results: Au $4f_{7/2} = 83.95 \pm 0.05$ eV and C $(1s) = 284.4 \pm 0.1$ eV for graphite. The materials under study were all oxide insulators and thus produced significant charging shifts, which were removed by using a low-energy electron flood gun. This procedure, described in detail elsewhere,[16] was successfully used in many related silicate studies.[17,18]

Results and Discussion

Initially, silica was deposited from an aqueous solution of sodium silicate diluted eight times in water (v/v) in the presence of sodium borohydride. The concentration of the reducing agent, sodium borohydride ($NaBH_4$), was 5 g/L. Deposition was performed at 75°C for 15 min. Subsequent to deposition, the samples were dried in air at room temperature for 24 h and then rinsed with distilled water. Visual observation showed a smooth, transparent glassy silica deposit. Figure 1a is a scanning electron microscopy (SEM) image of a galvanized steel panel coated with silica and shows well-defined hexagonal structures which are characteristic of zinc deposit. The silica coating reproduces the surface morphology of underlying zinc substrate, indicating the uniformity of the thin layer of silica deposit. Figure 1b shows the EDAX spectrum of the above-mentioned sample. The EDAX method was used to obtain a relative estimate of the silica deposited.[14] The average silica content in the deposit was found to be approximately 13.7 wt % with 86.3% being zinc. Linear polarization studies in a 0.5 M Na_2SO_4 (pH 4.0) solution were performed on several spots of the silicated sample to estimate the polarization resistance (Rp), also referred to as corrosion resistance. Figure 2 shows the linear polarization plot for bare galvanized steel and silica-coated galvanized steel. Also shown for comparison is the galvanized sample coated with a commercially available passivate such as dark yellow chrome. The polarization resistance measured by the linear polarization method for the silica-coated samples was 1432 Ω cm^2. The polarization resistance value is comparable to that of the silica deposit obtained by the electrolytic process.[14] Silica layers deposited using the electroless process are highly reproducible and have a 5 times higher polarization resistance than bare galvanized steel (286 Ω cm^2). Also, the resistance is comparable to that of commercially available passivates such as the dark yellow chrome (1539 Ω cm^2).

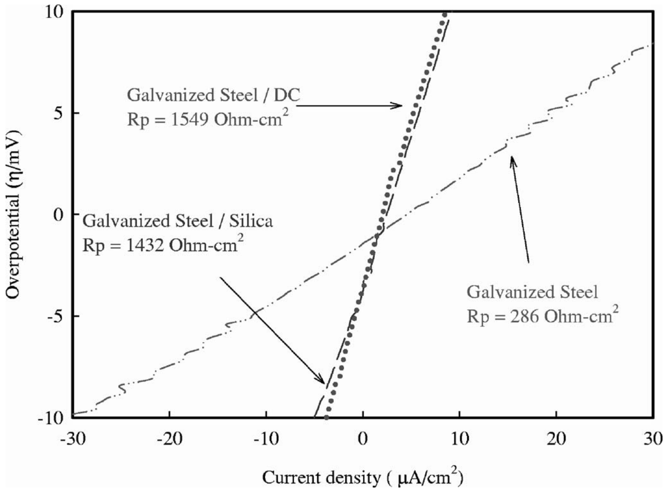

Figure 2. Linear polarization plot for bare galvanized steel, galvanized steels coated with silica, and dark yellow chrome.

The thickness and microstructure of the silica coating were analyzed by cross-sectional studies at high magnification under SEM. Figure 3 shows the cross-sectional SEM image of the galvanized steel panel coated with silica by the electroless process. A homogenous and dense silica layer tightly anchored to the zinc substrate is observed. The thickness of the silica layer deposited is approximately 500–600 nm. Also, the cross section reveals the presence of two distinct layers, a thin layer immediately over metallic zinc followed by a thick layer. ESCA studies were performed to analyze the metal–silicate interface and the deposition mechanism.

ESCA results and mechanism of silica deposition.— The coatings were characterized by using a variety of ESCA peak positions.[18,19] The resulting binding energy for the Si (2p) peak was the main basis for our study.[18] Figure 4a shows the Si (2p) binding energy spectrum obtained for the first thin layer over metallic zinc. Also shown in this figure is the ESCA spectrum for the bare galvanized steel. For the first layer over metallic zinc, the observed binding energy was close to 102.2 eV, which corresponds to Si found exclusively in a disilicate form.[18] The natural zinc disilicate, the hemimorphite form, has a binding energy of 101.8 eV. The value of

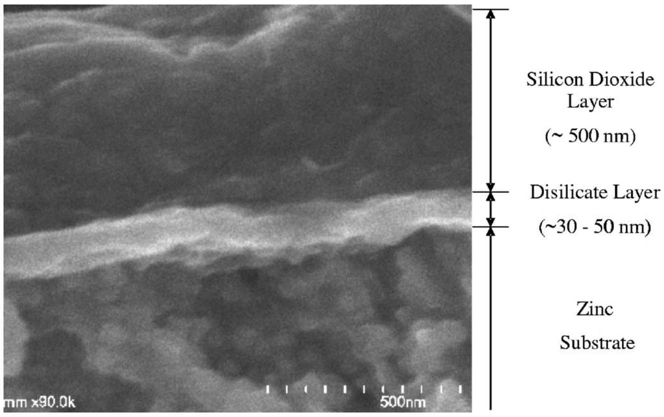

Figure 3. Cross-sectional view of the SiO_2 coating prepared by electroless process on a galvanized steel sample (magnification at 90.0 k).

102.2 eV observed in this study corresponds to disilicate species which exhibit Si (2p) orbital shifts as found in polymerized species.[17-19] A transition from monomeric to polymeric species results in a decrease of the covalency of the Si–O bonds, while the Si (2p) binding energy increases. Based on these results, the first layer corresponds to that of a thin zinc disilicate. The thickness of this layer is approximately 30–50 nm.

The formation of zinc disilicate can be explained through a simple adsorption process. SiO_2 dissolves in water to form monomeric $Si(OH)_4$ species. The amount of the SiO_2 hydrolyzed to $Si(OH)_4$ depends on the pH and temperature of the silicate solution. The equilibrium between SiO_2 and silica monomer is given by Eq. 1

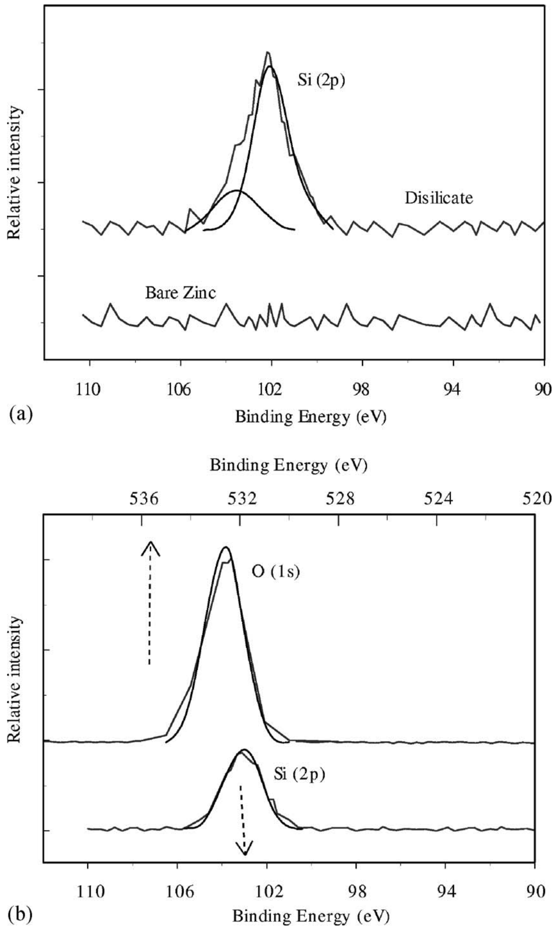

Figure 4. (a) Si (2p) ESCA spectra for the bare metallic zinc and the first layer over metallic zinc. (b) Si (2p) and O (1s) spectra for the second layer.

$$SiO_2 + 2H_2O = Si(OH)_4 \qquad [1]$$

According to Iler,[20] the monomeric species $Si(OH)_4$ condenses on any solid surface that bears OH groups with which it can react, namely, SiOH, or any MOH surface, where M is a metal that will form a silicate at the pH involved. In the present study, the Zn substrate is immersed in alkaline sodium silicate solution with a pH of approximately 10.5–11.0. Pourbaix diagrams show that zinc dissolves at this pH as zincate and bizincate ions.[21] The surface of the Zn substrate is covered with a thin layer of Zn hydroxide $Zn(OH)_2$. The monomeric $Si(OH)_4$ species react with the receptive surface to form zinc silicate by the following reaction

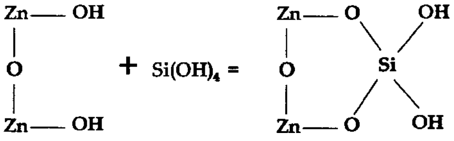

[2]

Thus, a thin layer of zinc disilicate is formed by an adsorption process and the reaction proceeds throughout the available receptive surfaces.

As shown in Fig. 4b, for the second layer, the binding energy of Si (2p) shifts to greater values of 103.3 eV, and 532.7 eV for O (1s), indicating the presence of SiO_2. The thickness of the SiO_2 layer is 500 nm. Once the receptive surface is covered by zinc disilicate, further growth of the silica is a molecular deposition of SiO_2. The mechanism for the molecular deposition of SiO_2 from $Si(OH)_4$ is a condensation reaction catalyzed by the presence of OH groups in which two silanol groups of silicic acid condense to form siloxane groups with the removal of water

$$-\underset{|}{\overset{|}{Si}}-OH + -\underset{|}{\overset{|}{Si}}-OH \longrightarrow -\underset{|}{\overset{|}{Si}}-O-\underset{|}{\overset{|}{Si}}- + H_2O \qquad [3]$$

Thus, the removal of water or the dehydration process catalyzes this reaction. In the electroless process the removal of the water at the interface takes place through the following reaction

$$NaBH_4 \rightarrow Na^+ + BH_4^-$$

$$BH_4^- + 2H_2O \rightarrow 4H_2 + BO_2^-$$

$$BO_2^- + Na^+ \rightarrow NaBO_2 \qquad [4]$$

The operating temperature of 75°C increases both the dehydration process and the kinetics of sodium borohydride decomposition. The condensation proceeds until a predominant amount of available silanol groups are used up for the production of siloxane bonds. The silicate formation is by an adsorption—condensation mechanism, which proceeds in two stages, namely: (*i*) formation of zinc disilicate by an adsorption process and (*ii*) condensation of the silicon dioxide over zinc disilicate.

The concentration of monomeric species, the rate of dehydration at the metal electrolyte interface, operating temperature, and pH of the bath are critical for the formation of uniform deposits. The role of the above parameters on uniformity and silica content in the deposit were studied to develop a corrosion-resistant silicate coating.

Effect of bath temperature.— Operating temperature of the bath plays a significant role in the deposition of silica. To analyze the effect of bath temperature, samples were prepared in a 1:8 sodium silicate/water solution with 5 g/L of $NaBH_4$ at various bath temperatures. Figure 5 shows the variation in the silica content and the polarization resistance of the coating deposited at various bath temperatures. The polarization resistance of the coatings was determined by linear polarization. The deposits prepared at room tem-

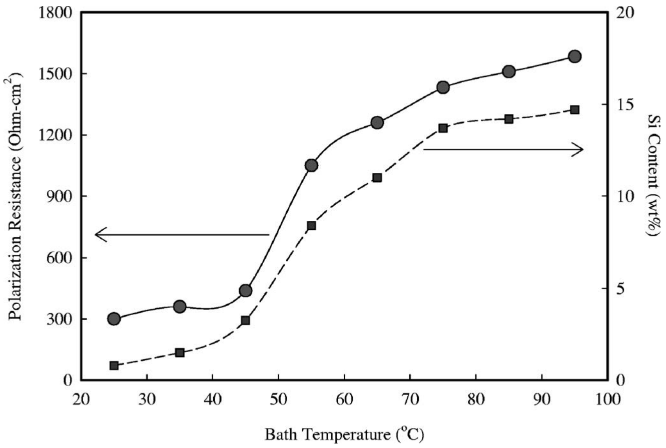

Figure 5. Average polarization resistance and silica weight percent of the deposits as a function of operating bath temperature. Deposition was done in 1:8 sodium silicate/water solution and 5 g/L of sodium borohydride.

perature (25°C) have a very low amount of silica (less than 1 wt %). By increasing the bath temperature, silica content increases and an optimum amount 14 wt% of silica was observed when deposited at a bath temperature of 75°C. Significant increase in the silica deposition was observed beyond a bath temperature of 50°C. This agrees with the previous findings of Iler[20] that silica formation is favored in hot solutions. Also, by increasing the bath temperature one increases the reaction rate of sodium borohydride, which catalyzes the silica deposition reaction. At temperatures higher than 75°C, no significant increase in silica content was observed. The polarization resistance for the deposit prepared at room temperature was 300 Ω cm^2, which is similar to that of a bare galvanized steel sample. Deposits prepared at 75°C show polarization resistance value of 1432 Ω cm^2. The observed increase in the polarization resistance is due to the formation of dense silica deposits.

Effect of pH.— The present inventive process is based on the formation of a passive film on the surface followed by adsorption of monomeric silica. Extensive studies exist on the passivation of zinc in alkaline sodium hydroxide and potassium hydroxide solutions.[22] In moderately alkaline solutions of pH 10.5, zinc forms passive films which reduce the rate of metal dissolution. Increasing the pH above 10.5 has a tendency to dissolve the passive film formed and increase active metal corrosion.[21] Figure 6 shows the open-circuit potentials (OCPs) of galvanized steel panels in 1:8 sodium silicate/water bath at different pH values. The temperature of the bath was 75°C. For the panel immersed in pH 10.5, the OCP values tend to more noble values due to the formation of passive film on the surface. With increase in pH, the formation of the passive film is affected and a less stable film is observed for a sample with pH 11.0. Further increase in pH to 12 leads to active dissolution of the zinc metal. This disrupts the formation of a uniform silica coating, especially the formation of the first zinc disilicate layer. The formation of poor silica film on the surface of the galvanized steel is reflected on the corrosion behavior of the coatings. Linear polarization study shows that for samples prepared at pH 10.5, the polarization resistance is 1432 Ω cm^2, in comparison with 720 Ω cm^2 for a sample prepared at pH 12.0. Also, the concentration of monomeric species, namely, $Si(OH)_4$, is a strong function of bath pH. The sodium silicate solution is a complex mixture of various silicate ions, such as $Si(OH)_4$, $HSiO_3^-$, SiO_3^{2-}, $Si_2O_5^{2-}$, $HSi_2O_5^-$, and $HSi_2O_6^{3-}$. Figure 6b shows the pH concentration diagram for various silicate species in equilibrium in sodium silicate solution. The concentration of various silicate species in the bath were determined by using several elemental balances and equilibrium conditions at a specified pH. The calculations are summarized and shown in the Appendix. Based on the calculations, we find that silica primarily exists as anions at pH greater than 10.0. At pH values lower than 10.0, the $Si(OH)_4$ concentration exceeds the solubility limit and becomes a gel. Experimental efforts to decrease the pH of the solution to less than 10.0 confirm this finding. Figure 6b shows that the concentration of $Si(OH)_4$ decreases with increase in pH and is negligible beyond a pH of 11.0. The concentration of $Si(OH)_4$ is crucial for the formation of an impermeable zinc disilicate layer followed by condensation of the SiO_2 layer. Thus bath pH should be maintained at a favorable value of 10.5 for two reasons: (*i*) formation of stable passive films and (*ii*) high concentration of $Si(OH)_4$ for the silica deposition to commence.

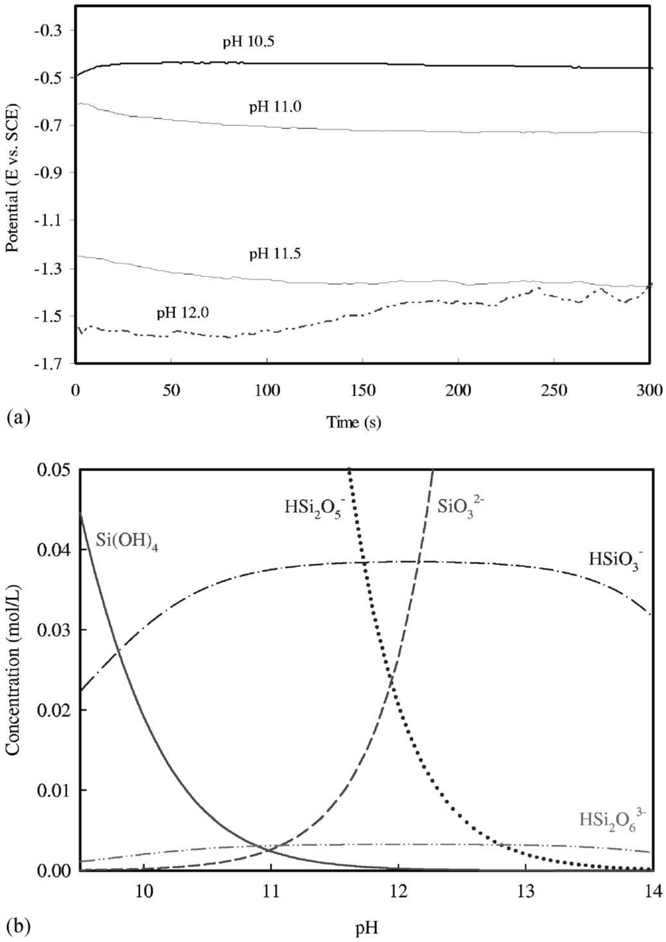

Figure 6. (a) OCP of galvanized steel panels immersed in 1:8 sodium silicate/water bath at different pH. (b) pH-concentration diagram for various silicate species in a sodium silicate solution.

Effect of sodium silicate concentration.— The successful formation of a uniform silicate layer on the zinc substrate is directly dependent on the amount of sodium silicate in the deposition bath. Different sodium silicate and water ratios such as 1:8, 1:5, 1:3, and 1:1 (v/v mix) were used to form the silicate layer. The depositions were performed for 15 min in the presence of 5 g/L $NaBH_4$ at a bath temperature of 75°C. Table I summarizes the average polarization resistance and silica content as a function of the sodium silicate concentration in the bath. The increase in thickness and the corresponding weight percent increase in the silica show that silica deposition is favored with increase in concentration of sodium silicate in the bath. The concentration of the monomeric species increases by increasing the concentration of sodium silicate in the solution, thus favoring silica formation. Silicate deposition with 1.5 μm thickness was obtained with use of a concentrated bath. Also, the polarization resistance of the deposit increases with concentration. The observed increase of polarization resistance is attributed to the increased

Table I. Effect of sodium silicate concentration on polarization resistance and Si content of deposits prepared by the electroless process.

Sodium silicate/ water	Silica content (wt %)	Polarization resistance (Ω cm^2)
1:8	13.7	1432
1:5	19.1	1661
1:3	24.87	1941
1:1	28.3	2057

Table II. Comparison of polarization resistance of deposits prepared by the electroless process with different concentrations of sodium borohydride.

Time (No. of days)	Polarization resistance (Ω cm^2)			
	0 g/L	3 g/L	6 g/L	9 g/L
Initial	1323	1870.1	1941.5	2168.9
1st day	632.1	1650.7	1660.2	2071.7
4th day	601.1	1072.1	1491.8	1856.2
7th day	560	830.1	1372.1	1590.1

amount of silica deposited. High polarization resistance of 2057 Ω cm^2 was obtained with the use of 1:1 sodium silicate/water solution. However, a 1:1 sodium silicate/water bath was more viscous, leading to difficulty in handling. Hence, a 1:3 sodium silicate/water bath was used for further studies. Another important observation made was the development of superficial microcracks as observed in SEM (not shown) for concentrations beyond 1:8 (sodium silicate/water). The amount of cracks formed was found to increase with increase in thickness of the silica deposited. The influence of these cracks on the corrosion resistance offered by silica coatings is discussed later.

Effect of sodium borohydride concentration.— The effect of sodium borohydride concentration on the coating performance was studied. The deposition was carried out on galvanized steel panels at 75°C for 15 min from 1:3 (sodium silicate/water) bath. The borohydride concentration was varied between 3 and 9 g/L. The treated samples were dried in air for 24 h and rinsed in distilled water. The surface coverage of silicate coatings for different concentrations of sodium borohydride was estimated using cyclic voltammetry (CV).

CV studies were done in a three-electrode setup using an SCE in 0.5 M Na_2SO_4, pH 4.0. The voltammograms were obtained by recording the current while varying the applied potential in the potential window of -1.6 to -0.8 V vs SCE. The scan rate was 5 mV/s. Figure 7 shows the CVs obtained for silicate samples prepared with different concentrations of sodium borohydride. The voltammograms obtained in comparison with bare galvanized steel are shown in the inset of Fig. 7. Because the currents depend on available bare surface of the substrate and it is proportional to the amount of material lost from the surface, CVs can be used to obtain a qualitative estimate for the inhibiting efficiency of silica coating toward corrosion. The peak reduction current and the maximum in the oxidation current decrease rapidly for silica-coated samples when compared to bare zinc samples. The observed large decrease in current in Fig. 7 is approximately 78% for 3 g/L and 92% for 9 g/L of borohydride. This indicates that the coating functions as a barrier film and decreases the dissolution of the underlying substrate significantly. Barrier protection of silica coating increases with the concentration of sodium borohydride.

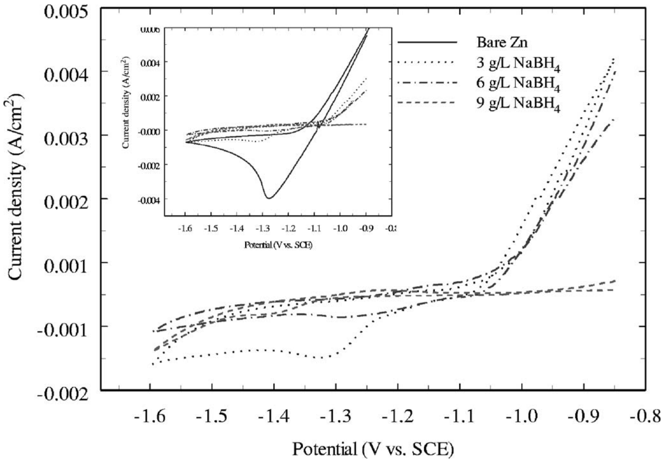

Figure 7. CVs of silica-coated samples prepared with different concentrations of sodium borohydride in a 1:3 sodium silicate/water solution. Comparison with bare galvanized steel panel is shown in the inset.

The sodium borohydride concentration was optimized based on the polarization resistance and stability of the coatings. The deposits were prepared from 1:3 sodium silicate/water electrolyte in the presence of different concentrations of sodium borohydride. To estimate the role of sodium borohydride, deposits were also prepared in the absence of sodium borohydride in the electrolyte. The polarization resistance was measured in a 0.5 M Na_2SO_4 solution, pH 4.0. After measuring the initial polarization resistance, the stability of the coating was tested by immersing the samples in distilled water for over a span of 1 week. The polarization resistance was measured at regular intervals and the values are summarized in Table II. The silica content was analyzed using EDAX before and after immersion in water for 1 week.

As shown in Table II, the polarization resistance and stability of the coating increases with the increase of the concentration of sodium borohydride. The samples prepared in the absence of sodium borohydride have initial polarization resistance of 1323 Ω cm^2, which is comparable to that of the chrome passivates. However, the stability of the coating in aqueous media is very low. The average polarization resistance drops to 630 Ω cm^2 after the samples were exposed in aqueous media for a period of 24 h. The samples prepared in the presence of 6 g/L of sodium borohydride have a polarization resistance of 1372 Ω cm^2, even after immersion in water for 160 h. The observed increase in stability of the deposits can be attributed to the removal of the water at the panel interface due to sodium borohydride decomposition, which enhances the condensation of the silica layer, thus forming dense silica films. This is evident from the values of the silica content measured initially and after immersion in water for 160 h which are presented in Fig. 8. As shown in Fig. 8, the silica weight percent in the deposit increases from 11.75% estimated for 0 g/L of sodium borohydride in the electrolyte to approximately 23% in the presence 3 g/L sodium borohy-

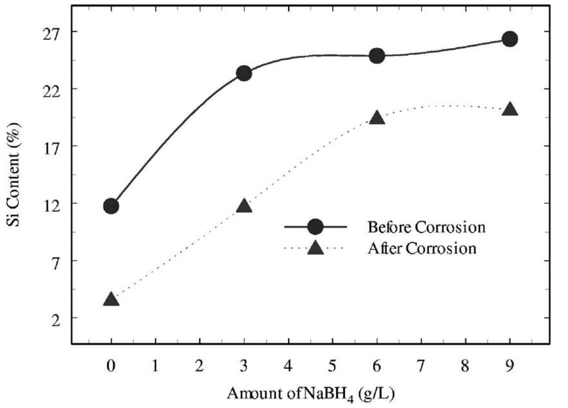

Figure 8. Silica content as a function of sodium borohydride concentration. Deposition was done in 1:3 sodium silicate/water solutions.

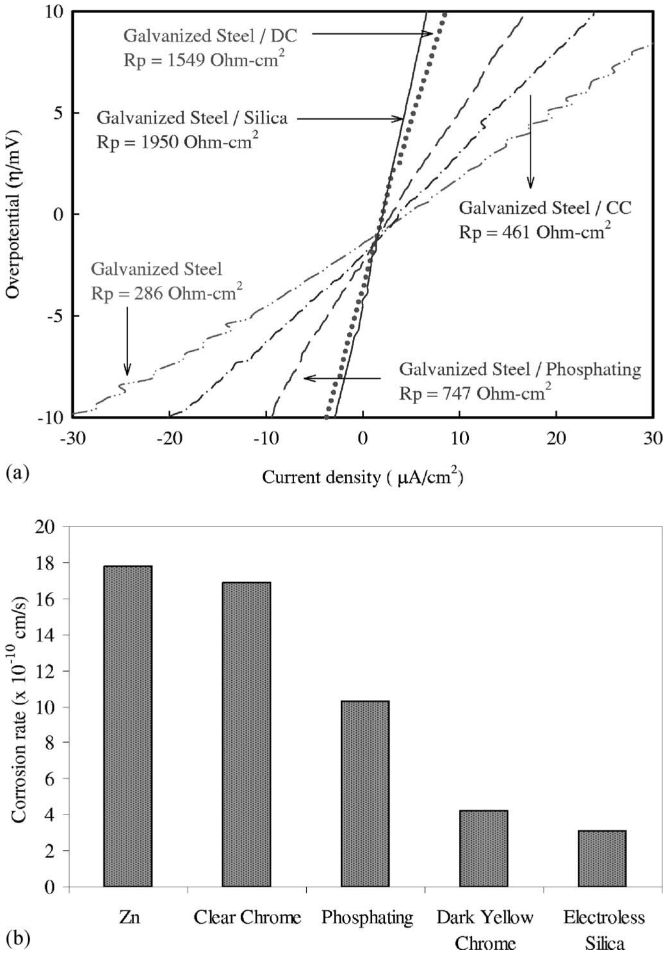

Figure 9. (a) Linear polarization plots for various coatings. (b) Comparison of corrosion rate of various coatings.

dride. For concentrations higher than 6 g/L sodium borohydride, as discussed above, the silica content in the deposit does not show any significant increase.

Corrosion performance in comparison with commercial coatings.— Since the objective of the present work is to substitute the toxic chromate processes with environmentally friendly coatings, it is imperative to analyze the corrosion properties of silica coatings and to compare them with the commercial passivation processes. Figure 9a shows a comparison of linear polarization responses obtained for electrogalvanized steel panels and electrogalvanized steel panels coated with conversion coatings such as phosphate, chrome passivates, and silica coatings prepared by the electroless method. The polarization resistance values are very low $(286\ \Omega\ \mathrm{cm}^2)$ for galvanized steel panels in the absence of conversion coating, indicating a rapid dissolution under corroding conditions. The highest polarization resistance values were estimated for silica coatings, indicating that these coatings have much better barrier properties when compared to the other commercial conversion coatings. The corrosion rate of these coatings is evaluated from the polarization resistance. The Stearn–Geary equation was used to evaluate the corrosion current and corrosion rate.[23] The estimated corrosion rates are shown in Fig. 9b. The low corrosion rates estimated for silica coatings suggest that these coatings are ideal for corrosion protection.

Salt spray testing was performed in order to evaluate the coating performance under accelerated corroding conditions. Table III summarizes the results obtained from the salt spray chamber study performed in compliance with ASTM B117 standards. The failure criterion was 5% surface coverage with red rust. Galvanized steel sample without any passivation or coating failed in a span of 48 h. Among the commercially available coatings, the passivation with dark yellow chrome showed better results compared to that of phosphating and clear chrome processes. With the yellow chrome process, the red rust appeared at 312 h, failing after 560 h, but on the control panels coated with silica coatings, the red rust appeared at 552 h, failing after 600 h. In the presence of a thin silica layer, the salt spray corrosion time extends to nearly 10 times over the untreated galvanized steel panel. A comparison of the corrosion data of the panels shows the improved performance of the silicon dioxide-based coating prepared by electroless method.

Table III. Results of ASTM B117 accelerated corrosion testing for various coatings.

	Time of exposure (hour)		
Coating	White rust	Red rust	Fail
Galvanized steel	24	48	48
Galvanized steel/phosphating	48	144	192
Galvanized steel/clear chrome	24	48	120
Galvanized steel/dark yellow chrome	144	312	560
Galvanized steel/silica	144	552	600

Corrosion and stability of silica coatings.— The silica deposited is porous in nature and is not impermeable. The stability of silica-coated panels in different media was tested through polarization resistance measurements. Two samples were immersed in 0.5 M Na_2SO_4 solution, pH 4.0, and distilled water. Another sample was left exposed in air. The polarization resistance was measured by linear polarization at regular intervals in a test solution of 0.5 M Na_2SO_4, pH 4.0. The depositions were performed in 1:3 bath for 15 min in the presence of 6 g/L $NaBH_4$ at a bath temperature of 75°C. Figure 10a shows the polarization resistance as a function of time of exposure. It is seen that samples exposed in air do not undergo any corrosion and the polarization resistance remains the same over a period of 1 week. However, for samples immersed in aqueous media, significant decrease in polarization resistance is observed. Figure 10b shows an SEM image of a silica-coated electrogalvanized steel panel before corrosion and after corrosion in water for 1 week. As mentioned before, superficial cracks were present for samples prepared from 1:3 bath. For the samples immersed in water for 1 week, white spongy particles were found on the surface of the coating. EDAX spot analysis shows that they are corrosion products of zinc. Despite the formation of corrosion products, the silica coating is still intact. Also the corrosion product does not proceed uniformly across the surface. They are predominantly found near the cracks. Unlike hexavalent chrome passivates, the silica coatings do not exhibit any self-healing mechanism. Instead, the corrosion products are expected to accumulate in the porous silicate coating, inhibiting further corrosion of the underlying zinc substrate. A similar phenomenon was also observed by Dalbin et al.[15] However, in the present case, the use of sodium borohydride produces dense silica films and offers improved stability for the silica coating. Despite the different protection mechanism, the silica coatings provide equivalent or better corrosion protection than chrome passivates, as observed from the salt spray chamber tests.

Conclusion

A novel nonchrome electroless process for the deposition of silica films has been developed. ESCA studies revealed that the coating is composed of two layers, an underlying zinc disilicate layer and a thick silicon dioxide layer. An adsorption–condensation mechanism is proposed to account for the two-layer silicate formation. Decomposition of reducing agent (sodium borohydride) catalyzes silica deposition by consuming water at the meta1–electrolyte interface. The operating parameters for the electroless process such as the concentration of the sodium silicate solution, operating tem-

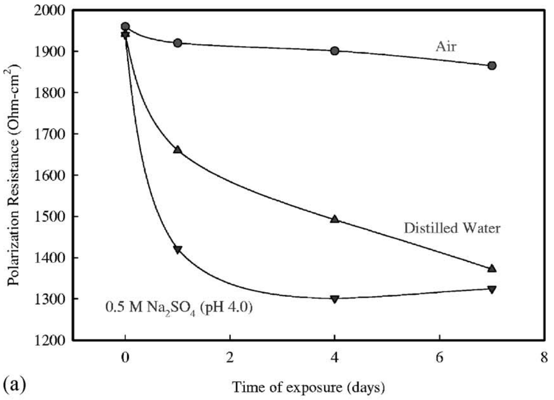

(a)

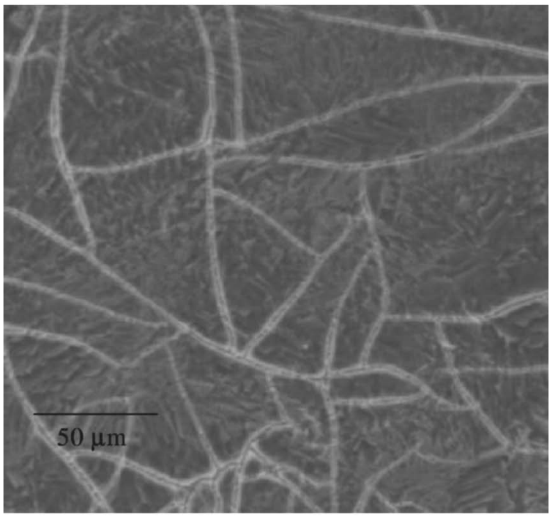

Before Corrosion

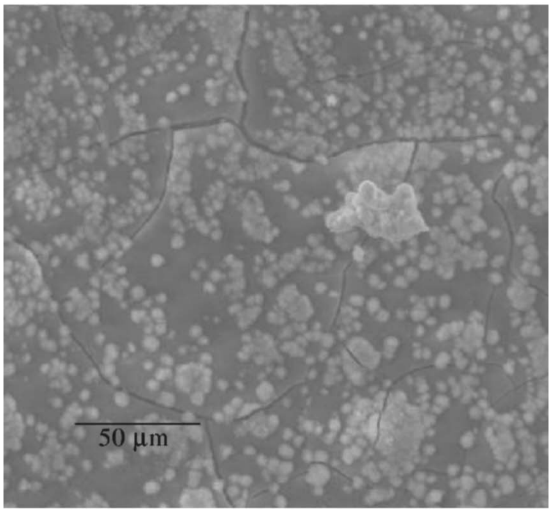

(b) After Corrosion

Figure 10. (a) Variation of polarization resistance of silica-coated galvanized steel as a function of time in various media. (b) SEM micrograph of silica-coated galvanized steel before and after immersion in distilled water for 1 week.

perature, and the amount of reducing agent (sodium borohydride) were optimized based on the corrosion protection performance of the coatings. Comparison of the corrosion data from the salt spray chamber shows the improved performance of the silicon dioxide coating compared to other commercially available conversion coatings. This process can also be applied to other substrates such as iron and aluminum.

Acknowledgment

Financial support by Elisha Technologies LLC, Office of Naval Research, and AESF is acknowledged. The authors also acknowledge Elisha Technologies for the ESCA and cross-sectional SEM studies.

The University of South Carolina assisted in meeting the publication costs of this article.

Appendix

The sodium silicate solution obtained from PQ Corp. is 37.5 wt % solution with SiO_2/Na_2O in a molar ratio of 3.22. The total silica concentration is 6.625 M. The silicate bath is a complex mixture of various species. The variables to be determined are as follows: $[Si(OH)_4]$, $[HSiO_3^-]$, $[SiO_3^{2-}]$, $[Si_2O_5^{2-}]$, $[HSi_2O_5^-]$, $[HSi_2O_6^{3-}]$. The concentration of the $[H^+]$ depends on the specified pH. The equations used to determine the equilibrium concentrations are:

Material balance on Si

$$[SiO_2] = [Si(OH)_4] + [HSiO_3^-] + [SiO_3^{2-}] + 2[Si_2O_5^{2-}] + 2[HSi_2O_5^-] + 2[HSi_2O_6^{3-}]$$

Equilibrium conditions $Si(OH)_4$ and $HSiO_3^-$

$$[H^+][HSiO_3^-] - k_1[Si(OH)_4] = 0$$

$HSiO_3^-$ and SiO_3^{2-}

$$[H^+][SiO_3^{2-}] - k_2[HSiO_3^-] = 0$$

$Si_2O_5^{2-}$ and $HSiO_3^-$

$$[Si_2O_5^{2-}] - k_3[HSiO_3^-]^2 = 0$$

$Si_2O_5^{2-}$ and $HSi_2O_5^-$

$$[H^+][Si_2O_5^{2-}] - k_4[HSi_2O_5^-] = 0$$

$Si_2O_5^{2-}$ and $HSi_2O_6^{3-}$

$$[H^+][HSi_2O_6^{3-}] - k_5[Si_2O_5^{2-}] = 0$$

These equations were solved simultaneously using Maple. The various rate constants used in the equations are as follows: $k_1 = 10^{-9.8}$, $k_2 = 10^{-12.16}$, $k_3 = 2200$, $k_4 = 10^{-9.8}$, and $k_5 = 10^{-12.8}$.

References

1. J. Flis, Y. Tobiyama, K. Mochizuki, and C. Shiga, *Corros. Sci.*, **39**, 1757 (1997).
2. L. Xia and R. L. McCreery, *J. Electrochem. Soc.*, **145**, 3083 (1998).
3. A. Suda and M. Asari Zairyo-to-Kankyo, *Corros. Eng.*, **46**, 95 (1997).
4. N. I. Sax and R. J. Lewis, Sr., *Dangerous Properties of Industrial Materials*, 7th ed., Vol. II, p. 745, Van Nostrand Reinhold, New York (1989).
5. J. A. Wharton, G. D. Wilcox, and K. R. Baldwin, *Trans. Inst. Met. Finish.*, **77**, 152 (1999).
6. M. F. Montemor, A. M. Simoes, M. G. S. Ferreira, B. Williams, and H. Edwards, *Prog. Org. Coat.*, **38**, 17 (2000).
7. J. C. Thresh, *Analyst (Cambridge, U.K.)*, **1922**, 459.
8. C. A. Vessey, C. Albon, and K. Holker, U.S. Pat. 3,706,603 (Albright and Wilson Ltd.) (1972).
9. J. J. Cox, Jr., U.S. Pat. 2,910,395 (Du Pont) (1959).
10. X. Cheng, Z. Wang, and Y. Yan, *Electrochem. Solid-State Lett.*, **4**, B23 (2001).
11. T. Jesionowski, *Colloids Surf., A*, **190**, 153 (2001).
12. E. A. Speers and J. R. Cohoon, *J. Electrochem. Soc.*, **145**, 1812 (1998).
13. M. Chigane, M. Ishikawa, and M. Izaki, *Electrochem. Solid-State Lett.*, **5**, D9 (2002).
14. B. Veeraraghavan, B. S. Haran, D. Slavkov, S. P. Kumaraguru, B. N. Popov, and B. Heimann, *Electrochem. Solid-State Lett.*, **6**, B4 (2003).
15. S. Dalbin, G. Maurin, R. P. Nogueira, J. Persello, and N. Pommier, *Surf. Coat. Technol.*, **194**, 363 (2005).
16. T. L. Barr, *Modern ESCA—The Principles and Practices of X-ray Photoelectron Spectroscopy*, CRC Press, Boca Raton, FL (1994).
17. H. He, T. L. Barr, and J. Klinowski, *J. Phys. Chem.*, **98**, 8124 (1994).
18. J. J. Hahn, N. G. McGowan, R. L. Heimann, and T. L. Barr, *Surf. Coat. Technol.*, **108**, 403 (1998).
19. T. L. Barr, *J. Vac. Sci. Technol. A*, **A9**, 1793 (1991).
20. R. K. Iler, *The Chemistry of Silica: Solubility, Polymerization, Colloid and Surface Properties, and Biochemistry*, John Wiley & Sons, NY (1979).
21. M. Pourbaix, *Atlas of Electrochemical Equilibria in Aqueous Solutions*, Sec. 15.1, Pergamon Press, New York (1966).
22. A. Macias and C. Andrade, *Br. Corros. J., London*, **22**(2), 113 (1987).
23. M. G. Fontana, *Corrosion Engineering*, 3rd ed., McGraw-Hill series in Materials Science and Engineering, Boston, MA (1986).